Philippine Journal of Science
152 (S1): 33-46, Philippine Meteorological Research
ISSN 0031 - 7683
Date Received: 26 Nov 2022

Spatio-Temporal Trend Analysis of Reference Evapotranspiration in Central Luzon, Philippines

Lea S. Caguiat[1]*, Ronaldo B. Saludes[2], Marion Lux Y. Castro[2], and Rubenito M. Lampayan[2]

[1]Institute for Climate Change and Environmental Management, College of Science, Central Luzon State University, Science City of Muñoz, Nueva Ecija 3119 Philippines
[2]Institute of Agricultural and Biosystems Engineering, College of Engineering and Agro-industrial Technology, University of the Philippines, Los Baños, Laguna 4031 Philippines

Understanding trends in reference evapotranspiration (ET_o) and their influencing factors is crucial for calculations of irrigation requirements and water management. Meteorological data in Central Luzon (1985–2019) were used to estimate ET_o using the FAO Penman-Monteith method. Spatial and temporal ET_o trends were analyzed using the Mann-Kendall test and Sen's slope estimator. Correlation and sensitivity analyses were conducted to analyze the impact of weather variables on ET_o. Positive correlations were observed for maximum temperature, solar radiation, and wind speed whereas negative correlations were observed for relative humidity and minimum temperature. In general, ET_o was statistically dependent and most sensitive to solar radiation, maximum temperature, and relative humidity. ET_o in the stations surrounded by mountains was consistently lower than the stations in the agricultural areas by 197 and 207 mm for the dry season and annual basis, respectively. The increasing trends with a magnitude of 3.98 mm/yr in annual ET_o were caused by the rising trend in solar radiation and maximum temperature and a decreasing trend in relative humidity. The decreasing ET_o trend (–2.6 to –4.63 mm/yr) predominant in the study area was mainly attributed to the decreasing trend of solar radiation and wind speed. Areas with increasing ET_o trends indicate the need for supplemental irrigation. Decreasing ET_o trends may indicate climate change, land-use change, or human-related factors.

Keywords: Central Luzon, FAO Penman-Monteith, reference evapotranspiration, trend analysis

INTRODUCTION

Evapotranspiration (ET) is a combination of two integrated processes where water is lost from soil and crop surfaces by evaporation and transpiration. It plays an important role in the heat and mass fluxes of the surface energy balance. One of the most common ET concepts is reference evapotranspiration (ET_o), which represents ET from a standardized vegetated surface, not short of water, at any given climatic condition (Allen *et al*. 1998). It is an important component of the hydrologic cycle that is computed from weather data. ET_o is used to estimate crop ET by integrating the crop coefficient (K_c). Analyzing ET_o trends is crucial as any change in meteorological variables due to climate change will affect the evaporative demand of the atmosphere changing the crop water requirements and water

*Corresponding author: lscaguiat@clsu.edu.ph

balance. Aside from meteorological variables, spatial and temporal trends in ET_o are affected by climate type, geographical location, environment, and land cover. ET_o trends have yielded a mixture of results across regions. Aschale *et al.* (2023) and Gul *et al.* (2021) highlighted the importance of quantitative estimation of the ET_o trend using long-term data, as it provides insights into water resource management and climate variability analysis.

Researchers established both increasing and decreasing ET_o trends. In Bangladesh, an "evapotranspiration paradox" was reported as the ET_o trends exhibited a decline of –1.19 mm/year in annual ET_o based on the data obtained from 18 meteorological stations for the period from 1980–2017 (Jerin *et al.* 2021). Despite the increase in mean temperature in the area, the decreasing trend still occurred due to the decrease in sunshine duration and wind speed. Spatial differences were also observed, as the southwest portion of Bangladesh has the highest annual values compared to the northwest. Similarly, Ndiaye *et al.* (2020) highlighted the existence of the same paradox in the Sahelian part of the Senegal River basin due to the decreasing wind speed and increasing relative humidity. In the Tarim River Basin in Central Asia, increasing ET_o trends were observed in spring, fall, and winter, whereas decreasing trends were reported in summer. Although results showed seasonal variations, the annual timescale still showed that mean ET_o was declining due to the decreasing wind speed. Changes in wind speed in the area were attributed to the combination of atmospheric circulation patterns, global warming, and human activities (Wu *et al.* 2021). Investigation of long-term ET_o trends from 1997–2017 in the sugarbelt area of the midlands of KwaZulu-Natal, South Africa revealed that decreasing ET_o trends in the majority of the area were caused by the changes in relative humidity and solar irradiance, highlighting the importance of local atmospheric condition studies to determine the causative factors (Ncoyini-Manciya *et al.* 2022). Decreasing precipitation was reported as the main culprit of the declining trend in ET_o over the Loess Plateau in China from 1982–2013. Areas with mean annual precipitation of 400 mm experienced decreasing trend, whereas areas with mean annual precipitation larger than 600 mm showed an increasing trend (Yang *et al.* 2016). Decreasing ET_o trends were consistently observed in mountainous areas. In northeast China, the results of the spatial and temporal variation analysis of ET_o demonstrate that there is a significant decreasing trend ($P < 0.05$) in mountainous regions (Song *et al.* 2018). Similar results were observed in India where a significantly decreasing ET_o trend occurred in mountain ranges. A decreasing trend in vapor pressure deficit and sunshine duration, which had a positive correlation to ET_o, was reported as the cause of the trend (Yadav *et al.* 2016). Several researchers also reported an increasing ET_o trend. Spatiotemporal trend analysis showed that higher annual average ET_o was observed in the south and east coastal area of South Korea in comparison to the northwest side. The majority of the stations reported a significant increasing trend, which was attributed to the increasing wind speed during autumn, early winter, and early summer, as well as increasing maximum temperature during spring and late summer (Hwang *et al.* 2020). In terms of potential ET, an investigation of climate data for the period of 1970–2022 in 56 stations across the Sichuan-Chongqing region, China reported an increasing trend in 58% of the weather stations considered. The positive trend was brought by the increase in vapor pressure deficit and the decreasing trends in wind speed and net radiation. Other research shows that important weather factors controlling ET_o are solar radiation (Ahmadi *et al.* 2022), temperature, RH, specific humidity, and wind speed (Wu *et al.* 2021; Aschale *et al.* 2023) The general objective of the study is to conduct a trend analysis of ET_o in Central Luzon, Philippines. It specifically aimed to [1] estimate ET_o using the FAO Penman-Monteith method; [2] determine the dominant weather variables affecting ET_o using the rank correlation coefficient and sensitivity analysis; and [3] analyze spatial and temporal trends of monthly, seasonal, and annual ET_o using the Mann-Kendall test and Sen slope estimator.

MATERIALS AND METHODS

Study Area

Central Luzon (Region 3) is a region of the Philippines that covers the provinces of Aurora, Bataan, Bulacan, Nueva Ecija, Pampanga, Tarlac, and Zambales. The region is situated between Northern Luzon and National Capital Region and lies from 119° 47' N to 122° 16' N and from 14° 21' E to 16° 31' E. Its total land area is 18,231 km^2 at an elevation of about 100 ft above sea level. Its slope (Figure 1) is mostly level and gently sloping with a steep slope in areas surrounded by Sierra Madre Mountains in the east, the Zambales Mountains in the south, and the Caraballo Mountains in the north. Figure 2 shows the climate map of Central Luzon based on the Modified Coronas' Climate Classification. The western part of the region has a Type 1 climate, whereas Aurora has a Type 2 climate. Some eastern portions of Bulacan and Nueva Ecija have a Type 3 climate. The soil type is alluvial which is very suitable for rice cultivation. The region is the leading producer of rice and is tagged as the "Rice Granary of the Philippines."

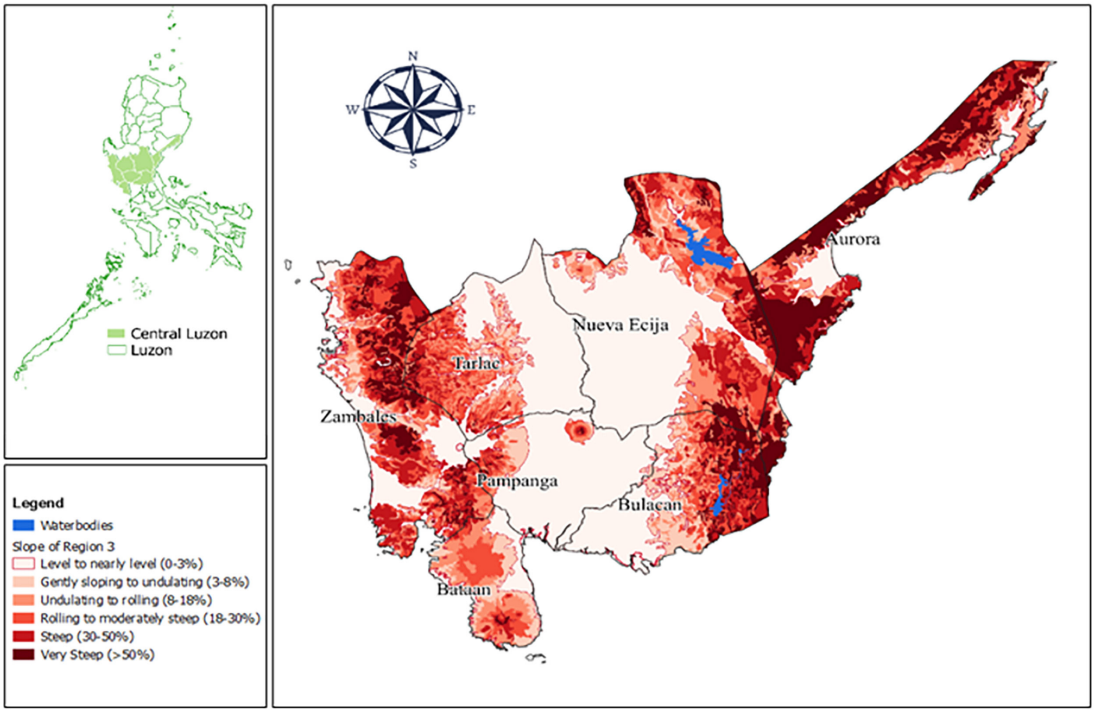

Figure 1. Central Luzon slope map (NAMRIA 2020a).

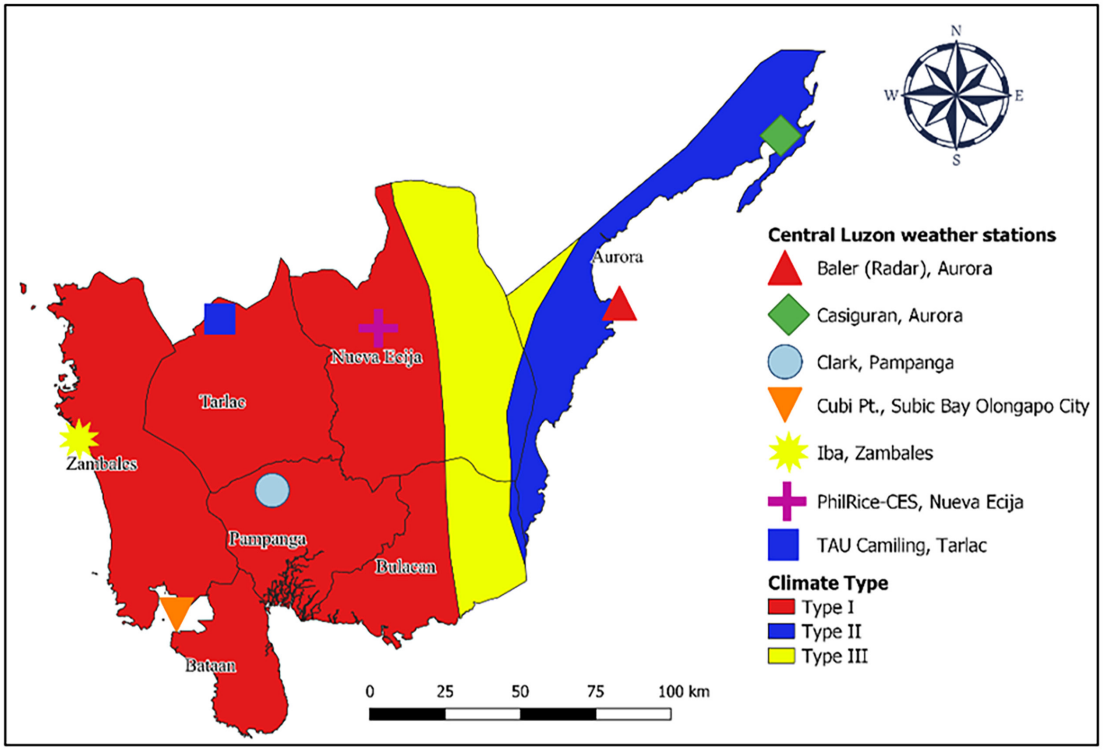

Figure 2. Climate type and weather stations in Central Luzon (NAMRIA 2020b).

Data Description

Daily meteorological records were collected from seven weather stations (Table 1) for available years between 1985–2019. The data were comprised of maximum and minimum air temperature, relative humidity, wind speed, and rainfall as provided by Philippine Atmospheric, Geophysical, and Astronomical Services Administration (PAGASA), Philippine Rice Research Institute (PhilRice), and Tarlac Agricultural University (TAU). The missing data were substituted with the corresponding long-term mean. The mean total annual rainfall in every station varies from 1756–3917 mm. Aurora is mainly covered by forests and small portions of wooded, natural, and cultivated lands, whereas Nueva Ecija, Tarlac, and Bulacan consist of cultivated and wooded lands with small sections of open forests. Pampanga is largely covered with cultivated lands and fishponds. Zambales and Bataan consist of well-distributed sections of natural, wooded, cultivated lands, and open forests. Weather stations in Aurora are situated in mountainous areas that are surrounded by forests and wooded lands, whereas the rest of the stations are in plains and agricultural areas that are surrounded by cultivated and natural lands. The land cover of Central Luzon is presented in Figure 3.

ET_o Estimation

ET_o was computed using the FAO Penman-Monteith method (Allen *et al.* 1998). Due to the lack of solar radiation data in most stations, solar radiation was estimated using the difference between the maximum

Table 1. Weather stations in Central Luzon, Philippines (PAGASA 2020).

Station name	Lat (°)	Long (°)	Elevation (m)	Duration
Baler (Radar), Aurora	15.75	121.63	173	1995–2018
Casiguran, Aurora	16.27	122.13	4	1985–2018
Clark Airport (DMIA), Pampanga	15.17	120.56	152	1998-–2018
Cubi Point, Subic Bay Olongapo City	14.79	120.27	19	1995–2018
Iba, Zambales	15.33	119.97	6	1985–2018
PhilRice-CES, Nueva Ecija	15.67	120.89	58	1987–2018
TAU Camiling, Tarlac	15.70	120.40	25	2011–2019

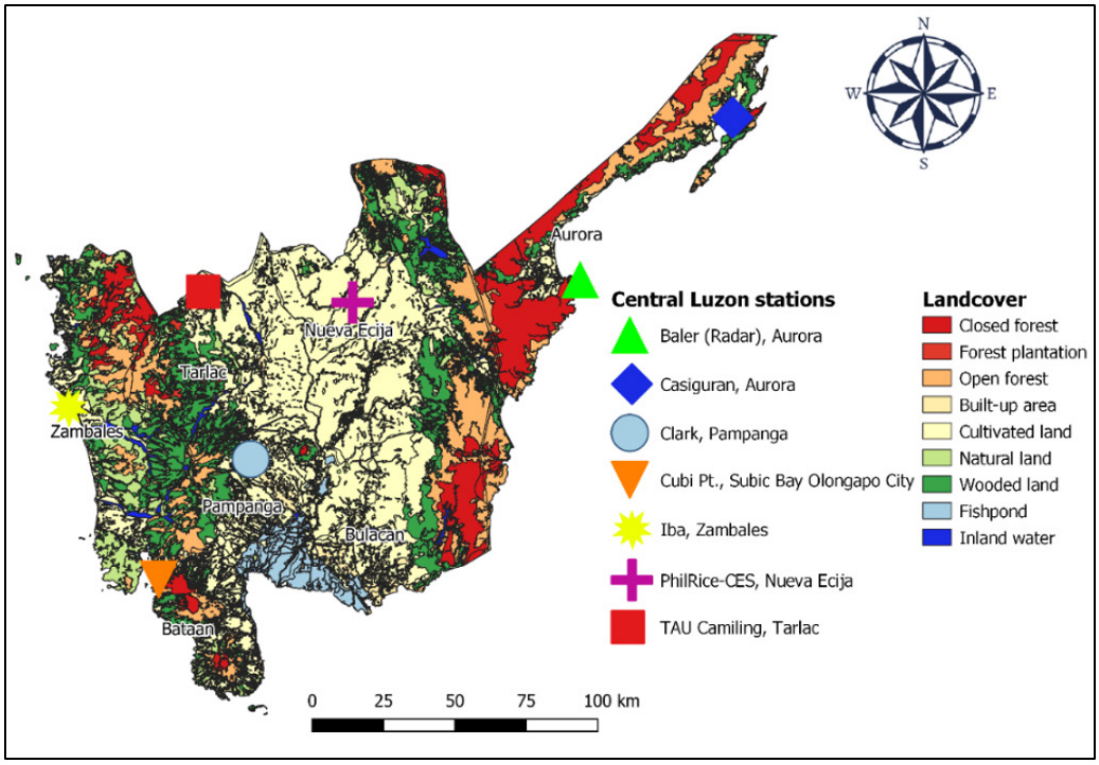

Table 1. Weather stations in Central Luzon, Philippines (PAGASA 2020).

and minimum temperatures. The weather variables were averaged over each month to get the mean daily monthly values. The mean daily monthly ET_o values were multiplied by the number of days in each month to provide a monthly estimate. Seasonal ET_o was obtained by summing the monthly ET_o values during the dry season (DS) from December–May and the wet season (WS) from June–November. Annual ET_o values were derived by summing monthly values in a year. The FAO ET_o calculator was used to facilitate the computations. ET_o was estimated using the equation:

$$ET_o = \frac{0.408\Delta(R_n - G) + \gamma\frac{900}{T+273}u_2(e_s - e_a)}{\Delta + \gamma(1 + 0.34u_2)} \quad (1)$$

where ET_o is the reference evapotranspiration (mm/d), R_n is the net radiation at the crop surface (MJ/m^2/d), G is the soil heat flux density (MJ/m^2/d), T is the mean daily air temperature at 2 m (°C), u_2 is the wind speed at 2 m (m/s), e_s is the saturation vapor pressure at the temperature of air (kPa), e_a is the actual vapor pressure (kPa), Δ is the slope of vapor pressure curve (kPa/°C), and γ is the psychrometric constant (kPa/°C).

Trend Analysis

The nonparametric Mann–Kendall test (MK test) and Sen's slope estimator were implemented using XLSTAT 2019.

Mann-Kendall (MK) Test

The MK test (Mann 1945; Kendall 1975), a widely used test for testing the significance of hydrometeorological trends (Ali and Abubaker 2019; Jerin *et al.* 2021; Ahmadi *et al.* 2022; Zheng *et al*. 2022), was used to analyze the trend of ET_o and the meteorological variables used to compute ET_o on a monthly, seasonal, and annual basis in every station. The test was based on the test statistics S defined as:

$$S = \sum_{i=1}^{n-1}\sum_{j=i+1}^{n} \mathrm{sgn}(X_j - X_i) \quad (2)$$

where, x_1, x_2, … x_n represent n data points, where x_j represents the data point at time j.

A very high positive value of S is an indicator of an increasing trend, and a very low negative value indicates a decreasing trend.

$$\mathrm{sgn}(X_j\_X_i) = \begin{cases} 1 \text{ if } (X_j\_X_i) > 0 \\ 0 \text{ if } (X_j\_X_i) = 0 \\ -1 \text{ if } (X_j\_X_i) < 0 \end{cases} \quad (3)$$

When n > 10, S becomes approximately normally distributed with mean E(S) = 0 and variance as:

$$VAR(S) = \frac{n(n-1)(2n+5) - \sum_{i=1}^{m} t_i(t_i-1)(2t_i+5)}{18} \quad (4)$$

where n is the number of data points, m is the number of tied groups (set of sample data having the same value), and t_i is the number of data points in the ith group.

Testing of trends was done at a specific significance level, α. Positive test statistic (Z) values indicate increasing trends, whereas negative Z values show decreasing trends. The standardized Z was computed as follows:

$$Z = \begin{cases} \frac{S-1}{\sqrt{VAR(S)}} \text{ if } S > 0 \\ 0 \text{ if } S = 0 \\ \frac{S+1}{\sqrt{VAR(S)}} \text{ if } S < 0 \end{cases} \quad (5)$$

Sen's Slope Estimator

Sen's nonparametric method often used to estimate the magnitude of trends in the data time series (Makwana *et al.* 2020; Ndiaye *et al.* 2020; Aschale *et al.* 2023) was computed by (Sen 1968):

$$\beta_i = \mathrm{Median}\left[\frac{x_j - x_k}{j-k}\right] \forall\ (k < j) \quad (6)$$

In this equation, x_j and x_k denote values data at time j and k, respectively, and time j is after time k ($k \le j$). The median of n values of βi is Sen's slope estimator test. A negative βi value represents a decreasing trend; a positive βi value represents an increasing trend over time. The N values of Qi are ranked from the smallest to the largest, and Sen's estimator is:

$$\beta_{med} = (\beta_{[(N+1)/2]}), \text{if N is odd} \quad (7)$$

$$\beta_{med} = \frac{1}{2}(\beta_{[N/2]} + (\beta_{[(N+2)/2]}) \text{ if N is even}$$

where β_{med} is tested by a two-tailed test at 100 (1−α) % confidence level.

MK Test with ESS Approach

The MK test with ESS approach by Yue and Wang (2004) was used, as it performs better when there are both a trend and an autocorrelation (Fathian *et al.* 2016; Hu *et al.* 2020). The variance $\sigma^2 s$ and the effective sample size n^* were given by:

$$\sigma^2{}_s = \sigma^2{}_s * \frac{n}{n^*} \quad (8)$$

$$n^* = \frac{n}{1 + 2 * \frac{\rho_1{}^{n+1} - n*\rho_1{}^2 + (n-1)*\rho_1}{n*(\rho_1 - 1)^2}} \quad (9)$$

where ρ_1 is the lag-1 autocorrelation coefficient computed after removing the trend:

$$x_k^* = x_k - \beta * (k-1), k = 1,2 \ldots, n \quad (10)$$

Rank Correlation Coefficient

Kendall's Tau correlation was performed to assess the impact of each weather variable on ET_o at a 5% significance level.

Sensitivity Analysis

The sensitivity coefficient (S) was computed to determine the changes in ET_o caused by the meteorological variables. The factors were changed within –20 and 20% at an interval of 1%. Using the first-order Taylor series approximation recommended by several researchers (Jhajharia *et al.* 2012; Li *et al.* 2017; Wu *et al.* 2021), S was calculated by:

$$S = \frac{\Delta ET_o}{\Delta X} \times \frac{|X|}{ET_o} \quad (11)$$

where S is the sensitivity coefficient, ΔX is the relative change of meteorological variable X, and ΔET_o is the relative change in ET_o induced by ΔX.

Geographical (Map) Analysis

Maps were established using QGIS 3.16.9. Maps were presented using point pattern analysis, which deals with the evaluation of spatial patterns of point features represented by weather stations.

RESULTS

Spatial Distribution of Seasonal and Annual Weather Variables

Solar radiation (Rs). The Rs of the stations surrounded by mountains were lower by 2.42 MJ/m^2/d compared to the stations in the agricultural areas. Minimal differences were observed for WS.

Air temperature. Large air temperature differences were observed in stations surrounded by mountains (Baler and Casiguran) than the stations in the agricultural areas during the DS, where the temperature was lower by 2.92, 0.97, and 1.96 °C for T_{max}, T_{min}, and T_{mean}, respectively. A similar scenario occurred during the WS, but minimal differences were observed. Similarly, the annual air temperature in the stations surrounded by mountains remained lower than the stations in the agricultural areas by 1.60, 0.61, and 1.11 °C for T_{max}, T_{min}, and T_{mean}, respectively.

Relative humidity (RH). The RH in stations surrounded by mountains have a higher magnitude (83–90%) compared to the stations in the agricultural areas (65–89%), depending on months. Similarly, the RH of the stations surrounded by mountains was observed to be higher than the stations in the agricultural areas by 12.69 and 3% for DS and WS, respectively. The same scenario occurred on an annual scale, wherein the RH remained higher in the stations surrounded by mountains by 7.8%.

Wind speed. Together with TAU and PhilRice, the stations surrounded by mountains (Baler and Casiguran) had low wind speeds (1–1.67 m/s). The rest of the stations had moderate wind speeds that ranged from 1.84–2.56 m/s. The lowest wind speeds occurred on the same stations with means of 1.44 and 2.38 m/s for DS and WS, respectively, whereas the rest of the stations had moderate wind speeds with means of 2.19 and 2.03 m/s for DS and WS, respectively.

Trend Analysis of Seasonal and Annual Weather Variables

Solar radiation. Positive trends were detected in Cubi Point and TAU with values ranging from 0.02–0.22 MJ/m^2. Except for Baler, the remaining stations had significant decreasing trends ranging from –0.06 to –0.09 MJ/m^2.

Air temperature. All stations had an increasing trend in T_{max} except for Casiguran during the DS. The significant increasing trends for T_{max} ranged from 0.02–0.17 and 0.02–0.12 °C on a seasonal and annual basis, respectively. All stations also resulted in significant positive T_{min} trends except for Baler and Iba, where the DS and annual basis were insignificant. The significant increasing trends for T_{min} ranged from 0.01–0.08 and 0.02–0.07 °C on a seasonal and annual basis, respectively.

Relative humidity. Baler and Iba resulted in increasing trends on a seasonal and annual basis. The magnitude of the increase ranged from 0.05–0.46% on a seasonal and annual basis. The remaining stations had significant negative trends with values ranging from –0.07 to –0.64% and from –0.08 to –0.17% on a seasonal and annual basis, respectively.

Wind speed. Stations in Baler, Cubi Point, Iba, and TAU showed negative trends on a seasonal and annual basis. All trends for these stations were significant except for TAU during DS and annual basis. The rest of the trends were mostly insignificant except for Casiguran, which showed significant increasing trends on a seasonal and annual basis.

Influence of Meteorological Variables on ET_o

Rank correlation coefficient. Table 2 shows the results of the correlation test on a seasonal and annual basis. Significant positive correlations were observed for T_{max}, Rs, and wind speed, whereas a negative correlation was observed for RH and T_{min}. In general, ET_o was statistically

Table 2. Kendall's Tau rank correlation coefficient of weather variables.

Station[a]	Variable[b]	Cool DS	Hot DS	WS	Annual
Baler	Rs	**0.813**	**0.850**	**0.804**	**0.855**
	RH	**–0.608**	**–0.602**	**–0.688**	**–0.717**
	T_{max}	**0.491**	**0.697**	**0.732**	**0.681**
	T_{min}	–0.110	–0.208	–0.022	–0.261
	Wind speed	0.110	0.062	0.145	0.087
Casiguran	Rs	**0.647**	**0.859**	**0.781**	**0.765**
	T_{max}	**0.573**	**0.534**	**0.428**	**0.547**
	T_{min}	**–0.247**	**–0.462**	**–0.393**	**–0.425**
	Wind speed	–0.186	**–0.329**	–0.161	**–0.272**
	RH	**–0.322**	0.029	–0.071	–0.107
Clark	Rs	**0.676**	**0.705**	**0.526**	**0.638**
	Wind speed	**0.476**	**0.524**	0.043	**0.448**
	T_{max}	**0.390**	**0.533**	**0.501**	**0.457**
	RH	**–0.543**	**–0.686**	**–0.415**	**–0.390**
	T_{min}	**–0.419**	–0.190	–0.062	–0.248
Cubi Point	Rs	0.188	**0.475**	**0.611**	**0.558**
	RH	**–0.507**	**–0.577**	**–0.531**	**–0.551**
	T_{max}	0.268	**0.461**	**0.647**	**0.514**
	T_{min}	–0.029	0.047	**0.291**	0.080
	Wind speed	**0.384**	0.258	–0.269	0.007
Iba	Rs	**0.483**	**0.616**	**0.668**	**0.668**
	T_{min}	**–0.372**	**–0.364**	**–0.344**	**–0.515**
	Wind speed	**0.483**	**0.423**	0.216	**0.462**
	RH	**–0.461**	**–0.453**	**–0.248**	**–0.283**
	T_{max}	0.111	**0.293**	0.216	0.127
PhilRice	Rs	**0.708**	**0.610**	**0.819**	**0.782**
	RH	–0.002	**–0.246**	–0.048	–0.056
	T_{min}	–0.071	0.044	–0.008	–0.040
	T_{max}	0.095	0.174	0.056	0.024
	Wind speed	0.228	0.012	–0.069	0.000
TAU	Rs	0.167	**0.638**	**0.944**	**0.857**
	RH	–0.222	**–0.754**	–0.278	**–0.786**
	T_{max}	–0.278	**0.638**	**0.667**	0.357
	Wind speed	**0.778**	0.457	0.222	0.143
	T_{min}	0.000	0.290	0.167	0.071

[a]The weather parameters are arranged in a decreasing order of correlation based on annual results
[b]The variable with a significant correlation to ET_o are marked in bold

dependent on Rs and air temperature on a seasonal and annual basis. Moreover, RH and Tmin also have a strong correlation to the ET_o at the stations in agricultural areas. In these areas, some variables showed a relatively strong correlation to ET_o at a specific season such as wind speed during the cool DS and RH during the hot DS.

Sensitivity Analysis

Figure 4 shows the curves determined by the sensitivity of ET_o to the weather variables. The sensitivity coefficient of ET_o in response to the 10% increment of the weather variables is shown in Table 3. Except for RH, the ET_o reacted co-directionally to the behavior of the rest of the

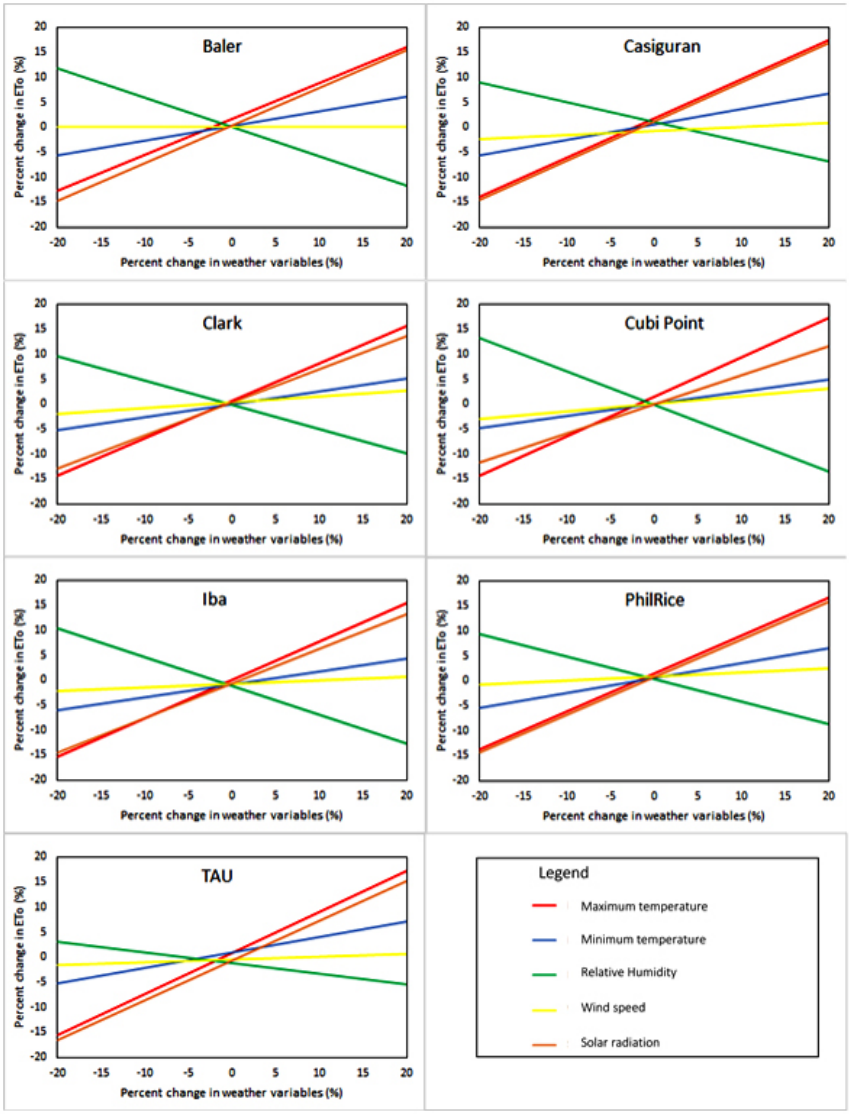

Figure 4. Sensitivity of ET_o to meteorological variables (%).

Table 3. Sensitivity coefficients of ET_o to meteorological variables.

Station[a]	Variable[b]	Cool DS	Hot DS	WS	Annual
Baler	Rs	0.75	**0.81**	**0.72**	**0.75**
	T_{max}	0.53	0.65	0.66	0.63
	RH	**–0.75**	–0.41	–0.62	–0.6
	T_{min}	0.21	0.24	0.29	0.26
	Wind speed	0	0.08	0.08	0.06
Casiguran	T_{max}	0.75	**0.67**	**0.61**	**0.66**
	Rs	0.73	0.6	0.56	0.61
	RH	**–0.85**	–0.23	–0.38	–0.46
	T_{min}	0.22	0.15	0.27	0.23
	Wind speed	0	0.16	–0.04	0.02

[a]The weather parameters are arranged in a decreasing order of sensitivity based on annual results
[b]The most sensitive variable affecting ET_o on a seasonal and annual basis are marked in bold

weather variables. In general, the sensitivity of weather variables to ET_o can be ranked as follows: T_{max}, Rs, RH, T_{min}, and wind speed.

Mean Monthly, Seasonal, and Annual ET_o Distribution

The spatial distribution of monthly, seasonal, and annual total ET_o values is presented in Figure 5. The ET_o distribution in a specific station was observed to be directly affected by the climate type, geographical location, and land cover in the area. The monthly ET_o at all stations reached their peak values in April and May (153–186 mm), whereas the lowest was observed mostly during December (84–116 mm). Results indicate that ET_o values recorded in the stations surrounded by mountains (Baler and Casiguran) were consistently lower than the stations in the agricultural areas and monthly differences in their values were between 3–63 mm. The pattern continued on a seasonal scale, where ET_o values at the stations surrounded by mountains remained lower during the DS by 197 mm. The same scenario was detected during the WS, but the differences were very minimal (10 mm). Annual total ET_o values reached 1446 and 1652 mm for the station surrounded by mountains and the stations in the agricultural areas, respectively. A similar pattern was detected on an annual scale, wherein the stations surrounded by mountains were lower than the stations in the agricultural areas by an average of 206 mm. Figure 6 shows the box plots of the ET_o values at all stations for every month. Significant seasonal differences can be observed among stations surrounded by mountains and stations in agricultural areas. For the stations in the agricultural areas, ET_o slowly increased during the DS and reached its peak during the hot DS (March–May) then gradually decreased during the WS. For the stations surrounded by mountains, the ET_o values are in a symmetrical distribution where the values slowly increased at the start of the month until they peaked from May–August then gradually decreased for the rest of the months. Annually, the rainfall exceeded ET_o for all stations, but a deficiency can be observed at the stations in the agricultural areas during the DS. The rainfall exceeds ET_o on a monthly, seasonal, and annual basis at the stations surrounded by mountains (Baler and Casiguran). On the contrary, a deficit of 347–572 mm was observed at the stations in the agricultural areas during the DS, as the ET_o exceeded the rainfall. The monthly, seasonal, and annual difference between rainfall and ET_o is shown in Figure 7.

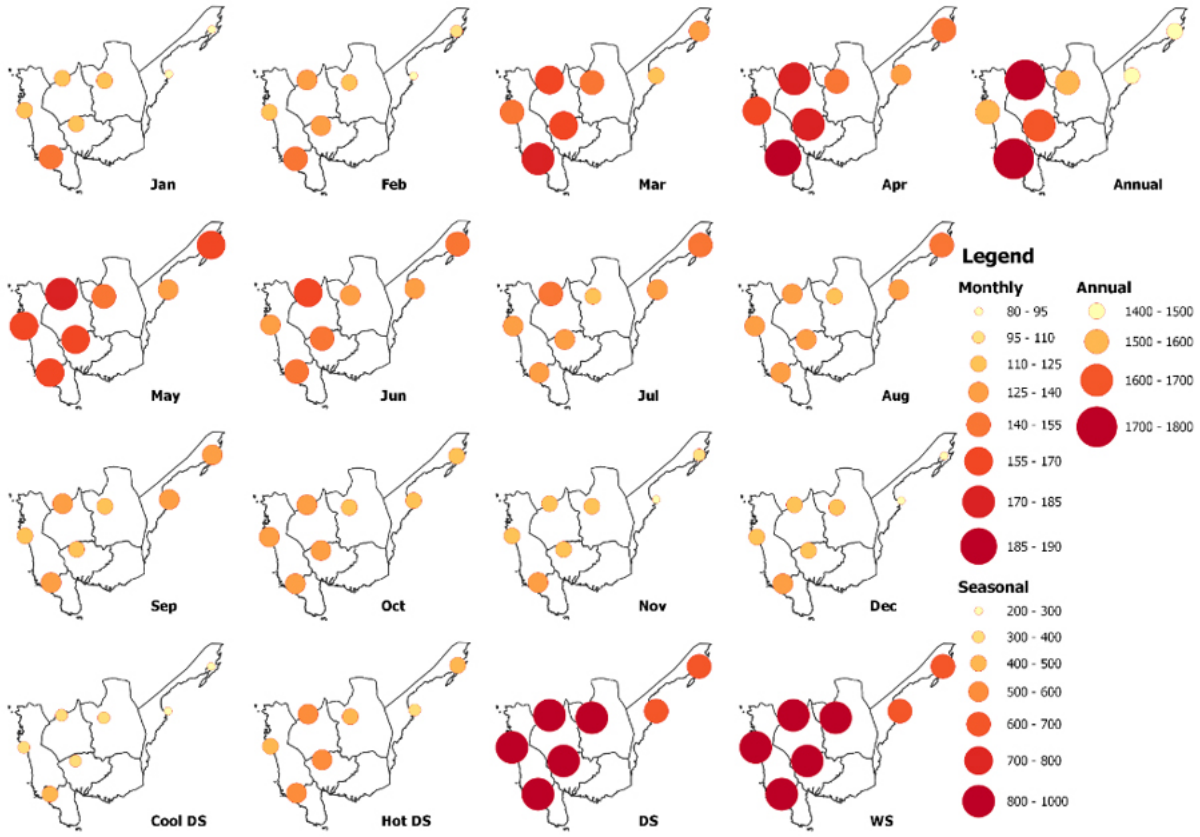

Figure 5. Spatial distribution of monthly, seasonal, and annual ET_o values (mm).

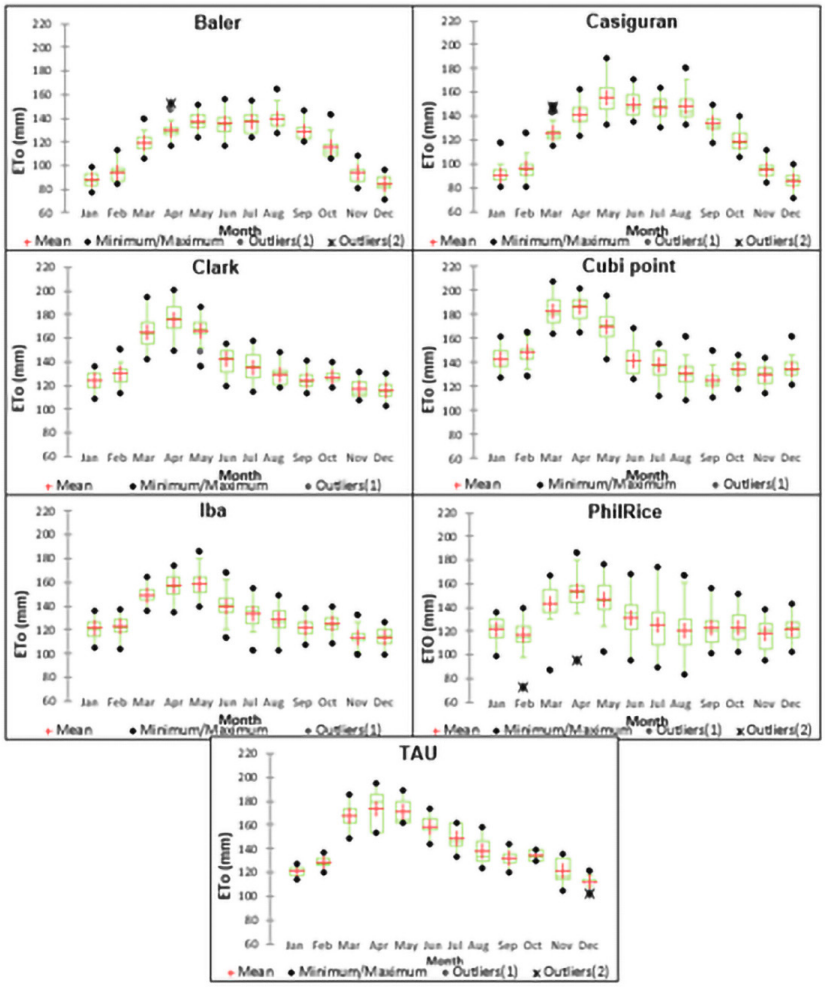

Figure 6. Box plots of monthly ET_o at all stations.

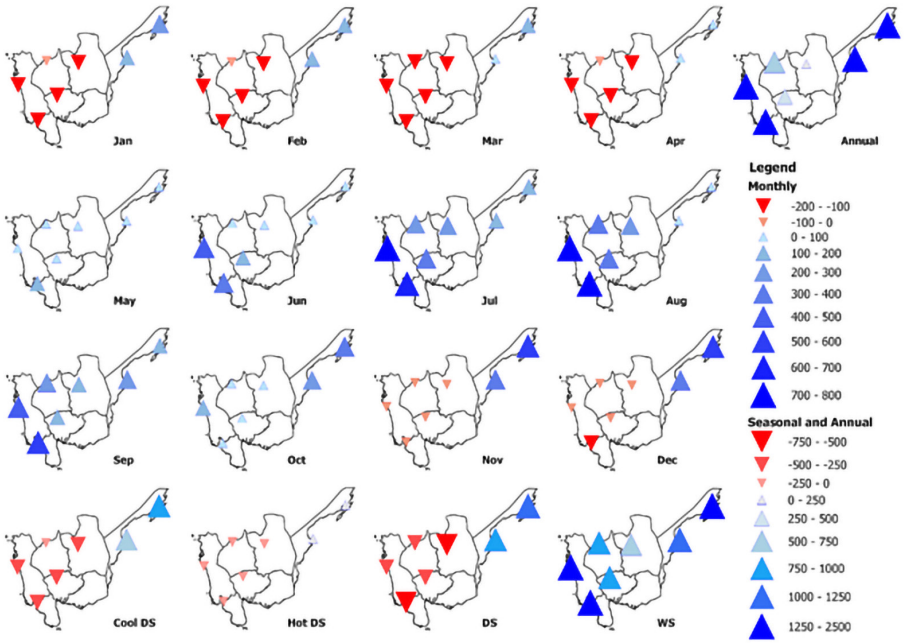

Figure 7. Monthly, seasonal, and annual differences in rainfall and ET_o.

Monthly, Seasonal, and Annual ET_o Trends

Results show that three stations (Casiguran, Iba, and PhilRice) had 7–12 mo of decreasing trend, wherein at least 5–11 mo were significant. The magnitude of the negative slope of monthly ET_o was between –0.07 and –1.74 mm/yr. Decreasing trends were also observed in Baler and Clark for 4 mo, whereas the rest of the months resulted in a no-trend condition. On the other hand, Cubi Point and TAU had more months (6–8 mo) of increasing ET_o trend with a magnitude of 0.21–2.40 mm/yr. Positive trends observed in Cubi Point were mainly significant, but trends in TAU were negligible.

Except for Cubi Point and TAU, a decreasing trend in ET_o was observed for all stations on a seasonal and annual basis. Positive trends observed in TAU were mostly insignificant except for the trend during the hot DS (6.2 mm/yr). The trends observed in Cubi Point were significant for hot DS (1.18 mm/yr), WS (1.73 mm/yr), and annual basis (3.98 mm/yr). The stations surrounded by mountains (Baler and Casiguran) both resulted in a decreasing ET_o trend. Trends observed in Baler were significant during cool DS (–0.38 mm/yr) only whereas trends detected in Casiguran were higher and significant during hot DS (–0.96 mm/yr), WS (–1.51 mm/yr), and annual basis (–2.60 mm/yr). A similar scenario was observed in Iba, PhilRice, and Clark, where the maximum decrease in the ET_o trend was observed. The magnitude reached –4.17, –4.63, and –2.29 mm/yr on an annual basis for Iba, PhilRice, and Clark, respectively. Table 3 and Figure 8 show Sen's slope and the spatio-temporal trends of ET_o on a monthly, seasonal, and annual basis.

DISCUSSION

Spatial differences in ET_o distribution were observed at the weather stations in Central Luzon. ET_o values recorded at the stations surrounded by mountains were consistently lower than the stations in the agricultural areas. Comparatively, lower ET_o in stations surrounded by mountains was caused by lower temperature (30.48 °C), higher RH (86.73%), and light wind speed (1.54 m/s). On the other hand, higher temperatures (32.08 °C), lower RH (78.90%), and moderate wind speed (1.80 m/s) were responsible for higher ET_o in the agricultural areas.

The shade, slope, aspect, and cloudiness in stations surrounded by mountains affected the spatial distribution of solar energy. Moreover, the temperature being lower at the stations surrounded by mountains was probably due to the differences in climate types. Lower temperatures may also be a direct effect of decreasing Rs brought by shading and cloudiness in areas surrounded by mountains. Moisture availability (RH and absolute vapor pressure) should have decreased in Baler (Moran 2018) and Casiguran, as they are surrounded by mountains; however, variability may have occurred on the windward and leeward sides of mountain ranges. As the air moves up the windward side of a mountain, it cools, and the volume decreases. Since stations in Baler and Casiguran have a Type 2 climate (no dry months) and are near inland waters as well, orographic clouds and precipitation mostly develop, which may have caused the increase of humidity in these areas. The wind being lower in mountainous areas resulted in a lower ET rate. The same scenario in Xinjiang, an autonomous region of China, was observed by Jia *et al.* (2022), wherein ET_o

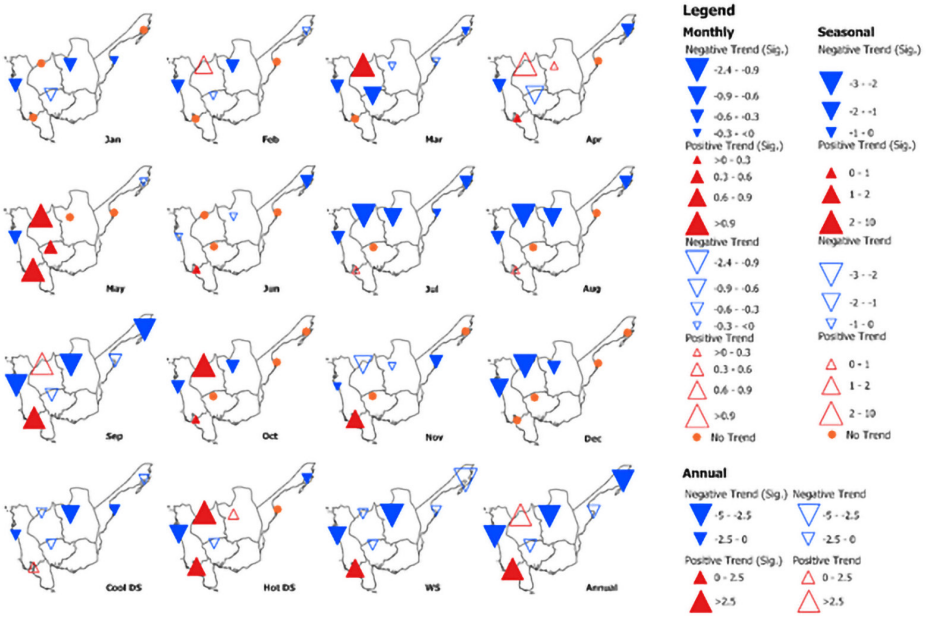

Figure 8. Monthly, seasonal, and annual ET_o trends (mm/yr)

values recorded were lower by 27.86 mm in high-elevation areas. Song *et al.* (2018) also detected that ET_o values in the mountainous areas were lower than the agricultural areas by more than 100 mm. Both increasing and decreasing ET_o trends were observed in the study area. The increasing ET_o trends were caused by the rising trend in Rs and T_{max} and a decreasing trend in RH. This implies global warming and drought (Hoegh-Guldberg *et al.* 2018; Zeng *et al.* 2019). On the other hand, the decreasing ET_o trend detected in the majority of the stations was mainly caused by decreasing trend of Rs and wind speed. A decreasing trend in Rs may indicate increasing cloudiness driven by shifts in atmospheric circulation and humidity (Dong *et al.* 2022). The decreasing trend in wind speed may be attributed to atmospheric circulation change (Xing *et al.* 2016), increased cloud cover, aerosols, and pollutants (Ndiaye *et al.* 2020), and human factors such as land-use change (Liu *et al.* 2022, 2019).

The ET_o trends were consistent with the result of the rank correlation coefficient and sensitivity analysis. For instance, the increasing ET_o trends observed can be explained by the rising trend in Rs and T_{max} and the decreasing trend in RH. These three weather variables were the dominant driving forces of the changes in ET_o in these stations based on correlation and sensitivity analysis. These results are consistent with the findings of Ahmadi *et al.* (2022) and Ndiaye *et al.* (2020), wherein the significant increasing trends in solar radiation and decrease in RH were the most influential factor for an increase in ET_o.

The significant decrease in RH was also the main driving factor of the increasing ET_o trend on the east coast of the Korean Peninsula (Ghafouri-Azar and Lee 2023).

The increasing trend of RH and T_{min} and the decreasing trend in wind speed observed in Baler caused the decreasing trend of ET_o since RH and T_{min} have a negative correlation to ET_o, whereas wind speed has a positive correlation. However, since wind speed and T_{min} in Baler both resulted in low correlation and sensitivity to ET_o, the trends were insignificant. The significant decreasing ET_o trend observed in Casiguran was caused by the significant decreasing trend of solar radiation detected in the area. Since the ET process is mainly dependent on solar energy, a significant decreasing trend in solar radiation was expected to largely influence the ET_o trend. Trend analysis of ET_o in Sicily (Aschale *et al.* 2023) and Bangladesh (Jerin *et al.* 2021) reported that the decreasing solar radiation was the main triggering factor of the negative ET_o trend. The significant decreasing ET_o trend detected in Iba, PhilRice, and Clark was caused by the decreasing trend of Rs in the area. In addition, a significant decreasing trend in wind speed in both seasons enhanced the decrease of ET_o in the area. Previous studies have also reported decreasing ET_o trends due to the decreasing trends in wind speed and solar radiation (Song *et al.* 2018).

CONCLUSION

ET_o distribution and trends revealed in this study provided information on the effects of climate type, geographical location, land cover, and trends in weather variables. It can provide insights to agricultural managers and stakeholders for irrigation scheduling and planning. The increasing ET_o trend caused by the rising trend in Rs and T_{max} and a decreasing trend in RH indicates the need for additional irrigation systems. The increasing trend indicates that climate change is pronounced in the area, particularly as ET_o also exceeds rainfall during the DS. Decreasing ET_o trends, caused by decreasing trend of Rs and wind speed that is found in the majority of the study area, may be a result of climate change, land-use change, or human-related factors such as urbanization and increasing construction works in the area.

ACKNOWLEDGMENTS

The study was funded by the Engineering Research and Development for Technology. PAGASA, PhilRice, and TAU were acknowledged as the providers of the weather data used.

REFERENCES

AHMADI A, DACCACHE A, SNYDER RL, SUVOČAREV K. 2022. Meteorological driving forces of reference evapotranspiration and their trends in California. Science of the Total Environment, 849: 157823. https://doi.org/10.1016/j.scitotenv.2022.157823

ALI K, ABUBAKER, K. 2019. Long-term Trends and Seasonality Detection of the Observed Flow in Yangtze River Using Mann-Kendall and Sen's Innovative Trend Method. Water 11(9): 1855. https://doi.org/10.3390/w11091855

ALLEN R, PEREIRA L, RAES D, SMITH M. 1998. Crop evapotranspiration: guidelines for computing crop water requirements. FAO Irrigation and Drainage Paper 56. Food and Agriculture Organization of the United Nations.

ASCHALE TM, PERES DJ, GULLOTTA A, SCIUTO G, CANCELLIERE A. 2023. Trend Analysis and Identification of the Meteorological Factors Influencing Reference Evapotranspiration. Water 15(3): 470. https://doi.org/10.3390/w15030470

DONG B, SUTTON RT, WILCOX LJ. 2022. Decadal trends in surface solar radiation and cloud cover over the North Atlantic sector during the last four decades:

drivers and physical processes. Climate Dynamics. https://doi.org/10.1007/s00382-022-06438-3

FATHIAN F, DEHGHAN Z, BAZRKAR MH, ESLAMIAN S. 2016. TRENDS in hydrological and climatic variables affected by four variations of the Mann-Kendall approach in Urmia Lake basin, Iran. Hydrological Sciences Journal. p. 1–13. https://doi.org/10.1080/02626667.2014.932911

GHAFOURI-AZAR M, LEE SI. 2023. Meteorological Influences on Reference Evapotranspiration in Different Geographical Regions. Water 15(3): 454. https://doi.org/10.3390/w15030454

GUL S, REN J, XIONG N, KHAN MA. 2021. Design and analysis of statistical probability distribution and non-parametric trend analysis for reference evapotranspiration. PeerJ 9: e11597. https://doi.org/10.7717/peerj.11597

HOEGH-GULDBERG O, JACOB D, TAYLOR M, BINDI M, BROWN S, CAMILLONI I, DIEDHIOU A, DJALANTE R, EBI KL, ENGELBRECHT F, GUIOT J, HIJIOKA Y, MEHROTRA S, PAYNE A, SENEVIRATNE SI, THOMAS A, WARREN R, ZHOU G. 2018. Impacts of 1.5 °C Global Warming on Natural and Human Systems. In: Global Warming of 1.5 °C. An IPCC Special Report on the impacts of global warming of 1.5 °C above pre-industrial levels and related global greenhouse gas emission pathways, in the context of strengthening the global response to the threat of climate change, sustainable development, and efforts to eradicate poverty. Cambridge University Press, Cambridge, UK and New York, NY, USA. p. 175–312. https://doi.org/10.1017/9781009157940.005

HU Z, LIU S, ZHONG G, LIN H, ZHOU Z. 2020. Modified Mann-Kendall trend test for hydrological time series under the scaling hypothesis and its application. Hydrological Sciences Journal 65(14): 2419–2438. https://doi.org/10.1080/02626667.2020.1810253

HWANG JH, AZAM M, JIN MS, KANG YH, LEE, JE, LATIF M, AHMED R, UMAR M, HASHMI MZ. 2020. Spatiotemporal trends in reference evapotranspiration over South Korea. Paddy and Water Environment 18(1): 235–259. https://doi.org/10.1007/s10333-019-00777-4

JERIN JN, ISLAM HMT, ISLAM, AR, SHAHID S, HU Z, BADHAN MA, CHU R, ELBELTAGI A. 2021. Spatiotemporal trends in reference evapotranspiration and its driving factors in Bangladesh. Theoretical and Applied Climatology 144(1–2): 793–808. https://doi.org/10.1007/s00704-021-03566-4

JHAJHARIA D, DINPASHOH Y, KAHYA E, SINGH VP, FAKHERI-FARD A. 2012. Trends in reference evapotranspiration in the humid region of northeast India. Hydrological Processes 26(3): 421–435. https://doi.org/10.1002/hyp.8140

JIA Y, SHEN X, YI R, SONG N. 2022. Spatial and Temporal Variability of ET_o in Xinjiang Autonomous Region of China during 1957–2017. Agriculture 12(9): 1380. https://doi.org/10.3390/agriculture12091380

KENDALL M. 1975. Rank Correlation Methods (4th Edition). London: Charles Griffin.

LI C, WU P, LI X, ZHOU T, SUN S, WANG Y, LUAN X, YU X. 2017. Spatial and temporal evolution of climatic factors and its impacts on potential evapotranspiration in Loess Plateau of Northern Shaanxi, China. Science of The Total Environment 589: 165–172. https://doi.org/10.1016/j.scitotenv.2017.02.122

LIU H, SONG D, KONG J, MU Z, ZHANG Q, WANG X. 2022. Spatiotemporal Variation in Actual Evapotranspiration and the Influencing Factors in Ningxia from 2001 to 2020. International Journal of Environmental Research and Public Health 19(19): 12693. https://doi.org/10.3390/ijerph191912693

LIU Z, DONG Z, ZHANG Z, CUI X, XIAO N. 2019. Spatial and temporal variation of the near-surface wind regimes in the Taklimakan Desert, Northwest China. Theoretical and Applied Climatology 138(1–2): 433–447. https://doi.org/10.1007/s00704-019-02824-w

MAKWANA JJ, DEORA BS, PARMAR BS, PATEL CK. 2020. Trend analysis in reference evapotranspiration using Mann-Kendall and Spearman's Rho tests in semi arid region of North Gujarat. Journal of Soil and Water Conservation 19(2): 170. https://doi.org/10.5958/2455-7145.2020.00023.5

MANN HB. 1945. Nonparametric Tests against Trend. Econometrica 13(3): 245. https://doi.org/10.2307/1907187

MORAN D. 2018. How Do Mountains Affect Precipitation? https://www.dtn.com/how-do-mountains-affect-precipitation/

[NAMRIA] National Mapping and Resource Information Authority. 2010. Geology of the Philippines (Land Cover 2010). https://www.philgis.org/

[NAMRIA] National Mapping and Resource Information Authority. 2020b. Philippines Climate Type Base Map. https://www.geoportal.gov.ph/

[NAMRIA] National Mapping and Resource Information Authority. 2020a. Slope Classes Shapefile. https://www.philgis.org/

NCOYINI-MANCIYA Z, SAVAGE MJ, STRYDOM S, CLULOW AD. 2022. Long-term reference evapo-

transpiration trend and causative factors analysis in the sugarbelt area of the midlands of KwaZulu-Natal, South Africa. South African Journal of Plant and Soil 39(3): 204–212. https://doi.org/10.1080/02571862.2022.2069874

NDIAYE PM, BODIAN A, DIOP L, DEME A, DEZETTER A, DJAMAN K, OGILVIE A. 2020. Trend and Sensitivity Analysis of Reference Evapotranspiration in the Senegal River Basin Using NASA Meteorological Data. Water 12(7): 1957. https://doi.org/10.3390/w12071957

[PAGASA] Philippine Atmospheric, Geophysical, and Astronomical Services Administration. (2020). Climatological data from DOST-PAGASA. http://bagong.pagasa.dost.gov.ph/climate/climate-data

SEN PK. 1968. Estimates of the Regression Coefficient Based on Kendall's Tau. Journal of the American Statistical Association 63(324): 1379–1389. https://doi.org/10.1080/01621459.1968.10480934

SONG X, ZHU K, LU F, XIAO W. 2018. Spatial and temporal variation of reference evapotranspiration under climate change: a case study in the Sanjiang Plain, Northeast China. Hydrology Research 49(1): 251–265. https://doi.org/10.2166/nh.2017.039

WU H, XU M, PENG Z, CHEN X. 2021. Temporal variations in reference evapotranspiration in the Tarim River basin, Central Asia. PLOS ONE 16(6): e0252840. https://doi.org/10.1371/journal.pone.0252840

XING W, WANG W, SHAO Q, YU Z, YANG T, FU J. 2016. Periodic fluctuation of reference evapotranspiration during the past five decades: Does Evaporation Paradox really exist in China? Scientific Reports 6(1): 39503. https://doi.org/10.1038/srep39503

YADAV S, DEB P, KUMAR S, PANDEY V, PANDEY PK. 2016. Trends in major and minor meteorological variables and their influence on reference evapotranspiration for mid Himalayan region at east Sikkim, India. Journal of Mountain Science 13(2): 302–315. https://doi.org/10.1007/s11629-014-3238-3

YANG Z, ZHANG Q, HAO X. 2016. Evapotranspiration Trend and Its Relationship with Precipitation over the Loess Plateau during the Last Three Decades. Advances in Meteorology. p. 1–10. https://doi.org/10.1155/2016/6809749

YUE S, WANG C. 2004. The Mann-Kendall Test Modified by Effective Sample Size to Detect Trend in Serially Correlated Hydrological Series. Water Resources Management 18(3): 201–218. https://doi.org/10.1023/B:WARM.0000043140.61082.60

ZENG Z, WU W, ZHOU Y, LI Z, HOU M, HUANG H. 2019. Changes in Reference Evapotranspiration over Southwest China during 1960–2018: Attributions and Implications for Drought. Atmosphere 10(11): 705. https://doi.org/10.3390/atmos10110705

ZHENG Q, HE J, QIN M, WU X, LIU T, HUANG X. 2022. Spatiotemporal variation of potential evapotranspiration and its dominant factors during 1970−2020 across the Sichuan-Chongqing region, China. PLOS ONE 17(6): e0268702. https://doi.org/10.1371/journal.pone.0268702